Title

CHARGE-EXCHANGE PRODUCTION OF ANTI-NEUTRONS AND THEIR ANNIHILATION IN HYDROGEN

Authors

Hinrichs, C. Keith
Moyer, Burton J.
Poirier, John A.
et al.

Publication Date

1962-02-05

UCRL-9589(2nd Rev)

University of California

Ernest O. Lawrence Radiation Laboratory

Berkeley, California

DISCLAIMER

UCRL-9589 (2nd Rev)

UNIVERSITY OF CALIFORNIA

Lawrence Radiation Laboratory
Berkeley, California

Contract No. W-7405-eng-48

CHARGE-EXCHANGE PRODUCTION OF ANTINEUTRONS AND THEIR ANNIHILATION IN HYDROGEN

C. Keith Hinrichs, Burton J. Moyer, John A. Poirier, and Philip M. Ogden

February 5, 1962

Charge-Exchange Production of Antineutrons and Their Annihilation in Hydrogen

C. Keith Hinrichs, Burton J. Moyer, John A. Poirier, and Philip M. Ogden

Lawrence Radiation Laboratory
University of California
Berkeley, California

February 5, 1962

ABSTRACT

The charge exchange of antiprotons into antineutrons and the subsequent annihilation of antineutrons have been studied in the 72-inch liquid hydrogen bubble chamber. The antiprotons were produced internally in the Bevatron; channeled externally by collimation, quadrupole focusing magnets, and bending magnets; and separated from other negatively charged particles by a system of three velocity spectrometers. Analysis of the data for a run with an antiproton momentum of 1.61 Bev/c has been completed. Three charge exchange reactions have been studied: (a) $\bar{p} + p \rightarrow \bar{n} + n$, (b) $\bar{p} + p \rightarrow \bar{n} + n + \pi^0$, and (c) $\bar{p} + p \rightarrow \bar{n} + p + \pi^-$. The cross section for Reaction (a) plus Reaction (b) was found to be strongly peaked forward with a value for the angular differential cross section at zero degrees of 4.6 ± 0.5 mb/sr. The total cross section for these two reactions was found to be 7.82 ± 0.55 mb. The total cross section for Reaction (c) was found to be 0.99 ± 0.24 mb; the statistical model would predict the cross section for (b) to be the same as (c).

Of the antineutrons produced in Reactions (a) plus (b), 122 annihilated in the bubble chamber; the resulting annihilation cross section was found to be 45.2 ± 5.4 mb. The kinetic energy of these antineutrons was distributed such that 80% of them had energies between 800 and 1000 Mev.

The average charged-pion multiplicity in the antineutron annihilations was found to be 3.5 ± 0.3. The ratio of the number of antineutron annihilations containing

five charged pions to the number containing three charged pions, and the momentum distribution of the pions, have been compared with predictions of a statistical model. Reasonable agreement was obtained for a volume five times that of a sphere with a radius of one pion Compton wavelength. The center-of-mass angular distribution of the pions in the antineutron annihilations was found to be, within statistics, an isotropic distribution. Three events were found that fitted K^0-meson production in antineutron annihilation.

Charge-Exchange Production of Antineutrons and Their Annihilation in Hydrogen*

C. Keith Hinrichs†, Burton J. Moyer, John A. Poirier,‡ and Philip M. Ogden

Lawrence Radiation Laboratory
University of California
Berkeley, California

February 5, 1962

I. INTRODUCTION

The antineutron was first identified by a counter experiment in 1956[1] after a few unsuccessful efforts to observe its existence, subsequent to the antiproton discovery. The antineutrons were produced by the charge exchange of antiprotons on protons ($\bar{p} + p \rightarrow \bar{n} + n$) and identified by their large annihilation energy in a counter. Other counter experiments have studied the charge-exchange reaction on hydrogen[2, 3, 4] as well as on complex nuclei,[5] and in 1959 the charge exchange of an antiproton into an antineutron and the subsequent annihilation of the antineutron were first observed in a propane bubble chamber.[6] In all these experiments it was assumed that the annihilation cross section for antineutrons was the same as that for antiprotons, in order to estimate the charge-exchange cross sections. In these previous experiments, the small value of the charge-exchange cross section, combined with the rarity of antiprotons themselves, permitted little more than confirmation of the process, and little light could be shed on the antineutron interactions, including annihilation.

The antineutron interactions in hydrogen are of particular interest because the reaction occurs in a pure isotopic spin triplet state, whereas the antiproton-proton interaction is composed of half isotopic singlet and half isotopic triplet states. It is to be noted that antiproton-neutron interactions also occur in the pure isotopic triplet state, and in this respect should be the same as $\bar{n}$-p interactions. Some recent results on antiproton-neutron interactions have been obtained by deuterium-hydrogen subtraction.[7]

The experiment presented here studies the antineutron-producing interactions of 925-Mev antiprotons in a 72-inch hydrogen bubble chamber, their angular distribution, and the nature of the antineutron-proton annihilation. The performance of this experiment was ancillary to an experiment that successfully searched for the antilambda in the reaction $\bar{p} + p \rightarrow \bar{\Lambda} + \Lambda$.[8,9] The energy of the experiment was dictated by the threshold for this latter interaction.

II. APPARATUS AND METHOD

A. The Antiproton Beam

The antiprotons were produced by the 6.2-Bev internal proton beam of the Bevatron striking an aluminum flip target. In the 200-ft space between the Bevatron and the 72-inch liquid hydrogen bubble chamber the antiprotons were focused, momentum-analyzed, and separated from a large background of pions, muons, and kaons by three velocity-selecting spectrometers. Time-of-flight counter techniques differentiated the antiprotons from pions and muons, and served as a monitor of the operation of the particle separators; their operation was further monitored by a matrix of counters which detected the position and distribution of the rejected pions. A counter telescope was also set up to look at 1-Bev/c pions coming from the same Bevatron target, and was used to monitor the operation of the Bevatron beam and target independently of the magnet and counter system of the main beam. A detailed description of the design of the antiproton beam has been published.[9] The composition of the beam as it entered the bubble chamber is discussed in Sec. III.

B. The 72-Inch Liquid Hydrogen Bubble Chamber

The bubble chamber is approximately 72 in. long by 20 in. wide by 15 in. deep[10] and is located in a magnetic field of 17.9 kgauss; the magnetic field varies in a known pattern by ± 10% over the volume of the chamber. The 1-msec Bevatron beam spill occurred at the center of the sensitive time of the bubble chamber, which

was about 15 msec, and at each expansion three cameras took stereoscopic pictures of the chamber. The magnetic field has been accurately measured over the volume of the chamber, and corrections for this variation as well as optical corrections have been made in the analysis of the data. The average density of the expanded hydrogen was 0.0586 g/cm^3.

III. ANALYSIS OF THE DATA

A. Classification of Reaction Types

The beam entering the bubble chamber was composed primarily of muons, antiprotons, and pions. The muons did not interact in the chamber and contributed only to the number of background tracks. The pions, although present in much smaller numbers, constituted the largest source of background for the antiproton interactions.

Table I lists the interactions with which we are concerned. They are classified by the charges of their final states since this feature is immediately determined by looking at the photographs. Reactions of beam particles in which no charged particles emerge are called 0-prongs; two charged emerging particles, 2-prongs, etc. A charged particle interacting with a proton must have a final state possessing an even number of charged particles, and a neutral particle interacting with a proton must have an odd number of particles in the final state; the presence of an incident beam track distinguishes the former from the latter. The scanning criteria used are described in Sec. III-B.

The experimental data presented here were directed toward the study of the antineutron production reactions (1), (2), and (6) and the antineutron annihilation reaction (13). The inelastic charge-exchange reactions producing more than one pion were presumed unimportant (for instance, no events were found to fit the reaction $\bar{p} + p \rightarrow \bar{n} + n + \pi^- + \pi^+$). Figure 1 is a photograph of a 0-prong antineutron production event, Reaction (1) or (2), followed by a 5-prong antineutron annihilation

event. A 2-prong antineutron production event which kinematically fits Reaction (6) is shown in Fig. 2--here the antineutron annihilates into three charged particles.

B. Scanning and Measurement of the Events

Approximately 46000 bubble chamber photographs were taken, with an average antiproton kinetic energy of 925 Mev. Each picture consisted of three stereoscopic views. They were rough-scanned on viewing reprojectors to locate possibly interesting events. A useful volume was defined for the bubble chamber which excluded areas where the film showed poor track visibility or where the proximity of a physical boundary reduced the probability of observing an interaction. Events were included in the analysis only if they were within this useful volume. About 6% of the pictures were rejected for reasons of quality, number of beam tracks, etc.

For a track to be considered a beam track it was required to: (a) enter the chamber at an angle within 5 deg of the average direction of the beam tracks, (b) have a curvature corresponding to a momentum of 1.6 ± 0.2 Bev/c, and (c) cross the entrance boundary to the useful volume.

An interesting neutral star was any interaction which did not contain: (a) an incident beam track, (b) a positively charged stopping track (which could only be a proton), or (c) one positive and one negative track (a V particle). Requirement (b) eliminated neutral events which could not have been annihilations. Many of the events which failed this test were recoil protons from neutron background, in which the proton later scattered another proton. Because of the large number of recoil protons relative to the estimated number of 1-prong antineutron annihilation events, the 1-prong events were not analyzed. For a similar reason no attempt was made to study Reaction (12). Scanning efficiencies for each type of event were determined by making two or more independent scans of the same film.

Accurate measurement of the events which were first found on the viewing projector were made on a digital measuring reprojector which recorded a succession of track coordinates in two of the three stereoscopic views.[11] An electronic computer program reduced these data (performing corrections for magnetic field nonuniformity and optical distortions) and printed out the momentum, angle, and position of each charged track, together with the errors in their determination.[12]

C. Determination of the Beam Composition

The total number of tracks in the 43100 pictures was, after correcting for the 5% scanning inefficiency, 191000. These tracks were due to antiprotons, pions, muons, and kaons. No attempt was made to distinguish these particle tracks by differences in bubble density, since they differed in this respect by only $\approx 2\%$. The number of kaons can be determined by their decay in flight, and is so small that it can be neglected. The muons are distinguished by their lack of interaction. The pions can be distinguished from antiprotons by the kinematics of delta-ray interactions; the maximum-energy recoil electron that can be produced by 1.61-Bev/c antiprotons is 3.7 Mev, whereas the corresponding delta-ray energy for pions of the same momentum is 125 Mev. The beam composition reported below was determined independently, but in essentially the same manner as that reported in an earlier reference[9], in which a more detailed discussion can be found. The average number of incident beam tracks was 4.4 per picture. We found that they were distributed in the following fashion: muons, 66% antiprotons, 24% pions, 10% and kaons, 0.05%.

D. Determination of the Number of Antineutrons Produced by the 0-Prong Process

We treat here the antineutron production from Reactions (1) and (2). Since these were the largest fraction of all 0-prongs, the number of antineutrons produced was obtained by subtracting the background 0-prongs from the total number. The total number of 0-prongs was determined to be 2149 ± 47; this number contains a

2% correction for the inefficiency of a multiple scan. The background 0-prongs were estimated to be: 453 ± 61 from pion reactions (4) and (5); 61 ± 54 from neutral antiproton annihilations, Reaction (3); and 11 ± 3 from antiproton production of $\Lambda\bar{\Lambda}$ pairs.[9] These values will be discussed below. Combination of these numbers gives a residue of 1624 ± 94, as the number of 0-prongs which yielded antineutrons.

The number of 0-prongs from pion reactions (4) and (5) was obtained from knowledge of the number of incident pions (Sec. III-C), the total pion-interaction cross section, and the ratio of the cross section for 0-prong production relative to the total cross section.[13] The 453 ± 61 0-prong events which were calculated in this fashion turned out to be the largest subtraction, and yet amounted to less than 1/4 of the total. Therefore the subtraction method should be quite valid.

The number of 0-prong antiproton annihilations, Reaction (3), was deduced as follows. The chamber photographs were scanned for electron-positron pairs associated with 0-prong events. The accepted pairs were required to display pair momentum directions passing through the 0-prong events; such pairs were considered to arise from conversion of decay photons coming from π^0s produced in the 0-prong events. On the basis of 32 such associated pairs, it was calculated, from the photon conversion efficiency of the chamber, that 946 ± 195 π^0's were produced by 0-prong events including Reactions (2), (3), (4), and (5). The π^0 yield from Reactions (4) and (5) was estimated from the π^-p interaction data of the Saclay group[14] to be 498 ± 81 (corresponding to the 453 ± 61 0-prong pion reactions mentioned above). The π^0 yield from Reaction (2) is deduced from the statistical model prediction that Reactions (2) and (6) should have about the same probability; in Sec. IV-D the pion yield of Reaction (6) is estimated from analysis of observations to be 205 ± 50, and this number is assigned to Reaction (2). Finally, then, by subtracting these estimated π^0 yields for Reactions (2), (4), and (5) from the total, we obtain 243 ± 217 as the

number of π^0's arising from 0-prong annihilations. Since the statistical model (see Appendix) predicts an average pion multiplicity of four for this mode, we conclude that the number of 0-prong annihilation events is 61 ± 54.

Another method to obtain the number of 0-prong antiproton annihilations is to calculate the number directly from the statistical model. If the volume parameter λ is taken to be 5 ± 1, then the number of 0-prong antiproton annihilations is calculated to be 212 ± 50. This number is considerably higher than the number obtained by the method above, although pion-pion resonances which are not included in the statistical model predication may be expected to reduce the number of 0-prong annihilations from that calculated by ignoring these processes. The number of 0-prongs which yield antineutrons would, on the basis of this latter calculated correction, be 1473 ± 94, instead of 1624 ± 94 as given in the first paragraph of this section.

E. Geometrical and Energy-Dependent Corrections

For each neutral star (defined in Sec. III-B) associated with a 0-prong, the probability P of the visible occurrence of the event was calculated. This probability is a function of the geometry of the bubble chamber as well as the position of the 0-prong and the angle of the antineutron, and is given by the equation $P = 1 - \exp(-\ell n \sigma'_{ann})$, where ℓ is the distance the antineutron could have gone before leaving the useful bubble chamber volume, σ'_{ann} is the cross section for antineutron annihilation into more than one prong, and n is the density of protons in the liquid hydrogen. No attempt was made to analyze 1-prong events since the number of proton recoils from neutron background was large compared to the expected number of antineutron annihilations into one-charge particles. A correction for this neglect is discussed below.

The weight W, where $W = 1/P$, for each event is the number of antineutrons that must have been produced at that particular angle so that the event would be seen.

The total number of antineutrons produced by 0-prongs that would annihilate into three or more charged pions would then be given by the sum of the weights for all of the associated events. This then allows us to calculate both the antineutron annihilation cross section (with a calculated correction for nonincluded 1-prong annihilations) and the angular distribution for the 0-prong charge-exchange cross section.

Smaller statistical errors are obtained if the probability P is averaged over position and azimuthal angle; this was done by a computer program. Given the position, direction, and momentum of the antiproton track at its beginning, this program reconstructed the track through the chamber. For each event a value of ℓ was determined (for the scattering angle θ of that event) for each of eight equally spaced azimuthal angles about the direction of the track at each of six equally spaced points along its reconstructed path. Each of these points along the track was weighted to account for the attenuation of the antiproton beam in passing through the chamber. Then P was determined for each ℓ and an average was performed.

Since it was not possible to scan for 1-prong annihilations, the calculated W gave only the number of antineutrons that would have annihilated into more than one charged pion. To correct for this, each W was multiplied by a factor K which was calculated from predictions of the statistical model for annihilation and the branching ratios for the various modes of annihilation [see Eq. (A-7) of the Appendix].

The antineutrons produced by Reactions (1) plus (2) had a distribution of energy which was peaked about 900 Mev (Fig. 3). To allow an energy dependence for the annihilation cross section, the formula of Koba and Takeda[15]

$$\sigma_{ann} = \pi (a + \lambda)^2 \qquad (1)$$

was used, where λ is the center-of-mass de Broglie wavelength for the antineutron

and a is a core radius. From Fig. 3 we see that 80% of the antineutron energy distribution lies between 800 Mev and 1000 Mev; the above form of the annihilation cross section varies by less that ± 3% within this energy interval. This introduces a slight energy dependence into W. Also, K is very slightly energy dependent; its energy dependence is discussed in Sec. IV-B.

IV. EXPERIMENTAL RESULTS

A. Number and Classification of Neutral Stars Associated with 0-Prongs

If a neutral star were associated with a 0-prong, it must occur in the forward hemisphere with respect to the 0-prong. (It is kinematically impossible for an antineutron to have a momentum component backward with respect to the antiproton in the laboratory frame of reference.) The number of false associations can be estimated in three ways: (a) from a scan of 5-prong or 7-prong stars occurring behind a 0-prong; (b) from the number of cases where more than one 0-prong could be associated with the same antineutron annihilation star; and (c) from the number of nonassociated antineutron stars, the number of nonassociated 0-prongs and the number of pictures. These estimates gave 5.4, 5.7, and 5.1, respectively, for the number of false associations. Thus the probability that a neutral star in the forward hemisphere of a 0-prong is associated is 0.956 ± 0.003. Thus there is a high probability, on statistical grounds alone, that a neutral star in the forward hemisphere of a 0-prong is associated with it.

Eighty-seven possible associations of 0-prongs with 3-prong stars were found. Of these, 83 occurred in the useful bubble chamber volume. The 3-prong stars of six of these events fitted π-p or p-p scattering; that is, the three tracks were coplanar and the momentum and energy balanced. (These events occurred for unassociated π's or p's that were not beam tracks.) Of the remaining 77 events, two could not be measured or analyzed accurately because of a missing stereo view or

because of obstruction of the event by bubble chamber hardware in one view. These two events appeared to be good in all respects, and since only six events were rejected previously out of 83, it was thought best to include them. Of the 75 measured events, all except one were found to be kinematically compatible with antineutron annihilation, with the $\bar{n}$ produced at the 0-prong. The one event that did not fit had too much visible energy in the star to have been produced by an $\bar{n}$ associated with the 0-prong. The event was assumed to be good, however, since one track in this event had a large error in momentum.

Fifty-one possible associations of 5-prong stars with 0-prongs were found; 44 occurred in the useful volume. All the measureable events were compatible with antineutron annihilation, the antineutron having been produced at the 0-prong; however, six of the 44 events were unmeasurable. All six unmeasurable events appeared to be good in all respects and were included. Only one association of a 0-prong with a 7-prong star was found, and it was compatible with antineutron production at the 0-prong.

The 83 three-prong events associated with a 0-prong star discussed above were classified as to the reliability of their annihilation interpretation. The stars were first analyzed as if they were scattering events; coplanarity was tested; all nearly coplanar events were then tested for energy and momentum balance, assuming a proton-proton scattering interpretation or various combinations of pion-proton scattering. As mentioned above, six events were found to be of this type. The remaining events were then analyzed to see if the visible energy of the neutral star was greater than 1 Bev. Various particle assignments were attempted (e.g., up to two proton tracks were permitted); if the minimum kinetic energy obtained from the various particle assignments was 1 Bev or more, it was assumed that the star could only be an annihilation event. Twenty-one events fitted these criteria. The next classification included 9 events in which the minimum visible energy was less than 1 Bev, but more than the kinetic energy of a neutron which came from the associated 0-prong.

A third classification was given to those events in which the minimum visible energy plus the minimum energy required to balance momentum was greater than 1 Bev (the balance of momentum assumed that the neutron was produced at the associated 0-prong). Forty-five events fitted these criteria. There remained two unmeasurable events.

The 44 five-prong stars were distributed so that 35 fitted the first criterion, three the third, and six were unmeasurable. There was one 7-prong star which fit the first criterion.

B. The Annihilation Cross Section

We calculated the ratio of 5-prong to 3-prong stars, using only those events which had an antineutron laboratory-frame kinetic energy between 800 and 1000 Mev. In this range there were 33 five-prongs and 63 three-prongs, which gave a ratio $R = 0.52 \pm .11$. The average kinetic energy for the 96 events was 894 Mev. This ratio is plotted in Fig. 4, along with predictions of the statistical model, as a function of antineutron kinetic energy, for various values of the volume parameter λ (see Appendix). A fit is obtained for $\lambda = 5 \pm 1$. A similar value of λ has been obtained from an analysis of the antiproton annihilation data.[16] With this choice of λ, the correction factor for 1-prong annihilation, K, was calculated as a function of antineutron laboratory-frame kinetic energy, and is plotted in Fig. 5. Since the antineutron energy is determined, an appropriate value for K could be chosen for each event. Then $\sum_i K_i W_i$ is the total number of antineutrons produced by 0-prongs when corrected for scanning efficiency and false associations:

$$N_0^{\bar{n}} = \frac{1}{\text{Efficiency}} \left(\frac{\text{Total - False}}{\text{Total}} \right) \sum_i K_i W_i, \qquad (2)$$

where $N_0^{\bar{n}}$ is the number of antineutrons produced by the 0-prong process.

The combined scanning efficiency for seeing annihilation stars associated with 0-prongs for 3-, 5-, and 7-prong stars was 0.975, and the number of false associations was taken to be 5.5. Putting these numbers into Eq. (2), with a correction to account for the fact that only 117 of the 122 events were measured and weighted, gives

$$N_0^{\bar{n}} = 1.021 \sum_{i=1}^{117} W_i K_i \,. \qquad (3)$$

The summation $\Sigma\ W_i\ K_i$ was determined for five values of the core radius, a, that is, a = 0.80, 0.85, 0.90, 0.95, 1.00 f, ($f = 10^{-13}$ cm). The actual value for $N_0^{\bar{n}}$ obtained in Sec. III-D is plotted as a line at $N_0^{\bar{n}} = 1624$, with errors ± 94. The intersection of the two curves occurs at a = 0.896. The values of the $N_0^{\bar{n}}$ obtained from both determinations are assumed to follow the Gaussian, or normal, error law. The ellipse in Fig. 6 is then the locus of points where the product of the probability amplitudes for the two distributions corresponds to the value at one standard deviation. The error in a is taken to be the maximum excursion of this ellipse parallel to the a axis. Thus, a = 0.896 ± .072, and from Eq. (1) the annihilation cross section at 900 Mev, obtained from 0-prong associated events is

$$\sigma_a\ (\bar{n} - p) = 45.2 \pm 5.4 \text{ mb.}^{17}$$

C. The 0-Prong Charge-Exchange Cross Section

The total cross section for charge exchange via the 0-prong mode was obtained from: (a) the number of antineutrons produced by the 0-prong process (1624 ± 94), (b) the total number of antiproton interactions which were observed (18728) and (c) the value for the total antiproton-proton cross section[18] corrected by 8% to account for unobservable small-angle scattering (90.2 ± 3 mb).

The deduced value for the total cross section for charge exchange from 0-prong reactions (1) plus (2) is 7.8 ± 0.6 mb.[17]

The differential cross section as a function of angle was obtained by summing the corrected weights for events in each interval of $\cos\theta$ and normalizing this sum to the total cross section,

$$\frac{d\sigma_{ce}}{d\Omega}(\cos\theta_j) = \frac{\left(\sum_k W_{kj}K_{kj}\right)\cos\theta_j}{\sum_j\left(\sum_k W_{kj}K_{kj}\right)\cos\theta_j} \cdot \frac{\sigma_{ce}\,(0\text{-prong})}{2\pi\,\Delta(\cos\theta_j)}, \qquad (4)$$

where θ is the center-of-mass angle between the $\bar{n}$ and $\bar{p}$ directions. This distribution is plotted in Fig. 7, together with the unweighted angular distribution of the 117 events. The extrapolated value at zero degrees is

$$\frac{d\sigma_{ce}\,(0\text{ deg})}{d\Omega} = 4.6\pm0.5\text{ mb/sr.}$$

D. The 2-Prong Charge-Exchange Cross Section

Since there were many more 2-prong interactions than 0-prong interactions, and since the cross section for Reaction (6), $\bar{p} + p \to \bar{n} + p + \pi^-$, is not expected to be large, there is a much higher statistical chance of an incorrect association of neutral stars with 2-prong vertices than in the previous case of 0-prong associations. However, there is an additional handle on these events since the kinematics of the associated event is over-determined. A computer program has been devised which adjusts the measured quantities of the 2-prong and the $\bar{n}$ direction under the constraints of energy and momentum conservation to give the best fit as determined by the smallest χ^2 value.[19]

This χ^2 test was performed on 85% of the data. There were 17 events for which

$\chi^2 \leq 15$; all others gave $\chi^2 \geq 200$. These 17 good events and three other events had been selected by a previous program. Due to measurement difficulties, the χ^2 test could not be performed for the other three events. The confirmation of the 17 events indicated that the three additional events should also be accepted.

The laboratory-frame kinetic energy of the antineutrons produced in these associated 2-prong interactions is plotted in Fig. 8 for 19 of the 20 events.

The sum of the weights for the associated events gave the number of reactions of this type that occurred. The cross section was then obtained from the relation

$$\sigma(p\bar{p} \to n\, p\, \pi^-) = \frac{\sum_i W_i \cdot \sigma_t'(\bar{p}p)}{\text{total number of observable } \bar{p} \text{ interactions}}, \tag{5}$$

where $\sigma_t'(\bar{p}p)$ denotes the total $\bar{p}p$ cross section corrected for the unobservable small-angle elastic scattering. The annihilation cross section for the antineutrons determined by Eq. (1) with a = 0.896 was divided by K to obtain a cross section for annihilation into more than one prong. This corrected annihilation cross section was used to determine the W_i for each of the 18 good events. For these events, $\Sigma W_i = 205 \pm 50$, corrected for a combined scanning efficiency of 0.99. By use of Eq. (5) we obtained[17]

$$\sigma(\bar{p} + p \to \bar{n} + p + \pi^-) = 0.99 \pm 0.24 \text{ mb}.$$

Of the 20 antineutron stars associated with 2-prong events, eight were three-prong stars, ten were five-prong stars and two were seven-prong stars.

The center-of-mass angles between the antiproton and the other particles of the 2-prong interaction are plotted in Fig. 9 for the 20 events that fit the reaction. The antineutron tends to go forward and the proton backward, with the pion having roughly an isotropic distribution. The distribution of antineutron azimuthal angle about the $\bar{p}$ direction is plotted in Fig. 10. Azimuthal zero is defined by the plane

of the proton and the antiproton.

E. The Nature of the Antineutron Annihilation Stars

As was mentioned in Sec. IV-B, the ratio of the number of 5-prongs to 3-prongs was observed to be $R = 0.52 \pm .11$ for the events that had an antineutron kinetic energy between 800 and 1000 Mev. For all 142 stars (122 0-prong association plus 20 2-prong associations), the ratio is $0.64 \pm .12$; the kinetic energy distribution for the antineutrons extends from 75 to 1100 Mev (average, 765 Mev). This point is indicated in Fig. 4 by the symbol (A). Eighty percent of the 0-prong star associations had an antineutron kinetic energy between 800 and 1000 Mev. Since the ratio R is a function of energy, the ratio calculated for the 96 events in this energy range was thought to be the more realistic value.

The average charged-pion multiplicity for the 142 stars was $3.8 \pm .3$. If an additional 12% in the number of stars due to 1-prong annihilation is assumed to exist, the multiplicity becomes $3.5 \pm .3$. The statistical model predicts that the number of charged pions is about twice the number of neutral pions, which would then imply that the total pion multiplicity was $5.2 \pm .4$. The statistical model (see Appendix) predicts a multiplicity of 5.1 for $\lambda = 5$, and 5.3 for $\lambda = 6$.

The pion momentum distribution determined in the c.m. of the $\bar{n}$ - p system is plotted for 3-prong stars in Fig. 11, and for 5-prong stars in Fig. 12. They are compared with the distribution predicted according to the statistical model for volume parameters $\lambda = 5$ and $\lambda = 6$. The areas of these curves are normalized to the numbers of pion plotted. Very good agreement is obtained for the 3-prong stars. Agreement is quite good for the 5-prong stars, but the observed distribution may peak at a slightly lower energy than that predicted. It should be noted that the momentum distribution is a relatively weak function of the statistical-model interaction volume.

The number of events available in these antineutron annihilations does not allow a statistically significant search for evidence of the two-pion and three-pion

resonant systems or "particles," such as can be profitably undertaken with the $\bar{p}$-p stars. However, we do observe the effect, usually attributed to Bose-Einstein statistics, of a somewhat closer angular correlation for pion pairs of like charge than for those of unlike charge. Thus if we evaluate the ratio of the number of pion pairs with included angle (in the c. m. frame of the annihilation) greater than 90 deg to the number with this angle less than 90 deg, we find this ratio to be 1.11 ± 0.15 for pions of like charge and 2.13 ± 0.24 for those of unlike charge. These numbers refer to the total of both 3-prong and 5-prong stars. Similar results have been previously noted and discussed for antiproton annihilations.[20, 21] However, the explanation of this effect purely in terms of the Bose-Einstein statistics, without the implication of any pion-pion interaction, requires a radius for the interaction volume too small to predict the observed pion multiplicities.

All the frames containing 3-, 5-, or 7-prong stars were scanned for a V pointing at the star. Only one event was found to fit a K^0 coming from a star, and this 3-prong star was not associated with either a 0- or 2-prong antineutron production. In addition, two V's were found that fitted a K^0 coming from a 1-prong annihilation. In one of these the antineutron came from a 2-prong beam track ending, and in the other the antineutron was produced by a 0-prong. For the latter case the 1-prong star and the 0-prong ending were only 2 deg apart as measured from the V. It was therefore uncertain whether the K^0 came from the 1-prong or was produced by the 0-prong. From these investigations it was possible only to say that we have some evidence for K production in $\bar{n}$-p annihilations, although the amount observed was perhaps less than expected by comparison with $\bar{p}$-p annihilation.

V. DISCUSSION

The value obtained for the antineutron annihilation cross section at 900 ± 83 Mev, $\sigma_{ann}(\bar{n}\text{-}p) = 45.2 \pm 5.4$ mb,[17] agrees within statistics with the antiproton annihilation cross section,[16] $\sigma_{ann}(\bar{p}\text{-}p) = 51 \pm 3$ mb. The $\bar{p}$-p annihilation is composed of half isotopic singlet and half isotopic triplet states, while $\bar{n}$-p annihilation is a

pure isotropic triplet state. The similarity of the annihilation cross sections indicates that the annihilation amplitudes for the singlet and triplet states are also similar.

It should be noted that in the determination of $\sigma_{ann}(\bar{n}\text{-}p)$, the energy for the $\bar{n}$ was assigned on the basis of Reaction (1), $\bar{p} + p \rightarrow \bar{n} + n$. It was estimated, however, that about 13% of the antineutrons were produced by Reaction (2), $\bar{p} + p \rightarrow \bar{n} + n + \pi^0$, and therefore 13% of the antineutrons would have a somewhat lower energy--more in keeping with the energy distribution for $\bar{n}$'s produced in 2-prongs (see Fig. 8).

The values used for K, the correction for 1-prong annihilation, were calculated from the predictions of the statistical model for $\lambda = 5$, which is consistent with that found in analysis of the ratio of the number of 2-, 4-, and 6-prongs in $\bar{p}$-p annihilation.[16] Fortunately, K is not a strong function of λ and decreases by only about 2% if, for example, λ is changed from 5 to 6. A more serious question is whether the statistical-model prediction of 12% for the 1-prong annihilation is in error.

The total inelastic cross section for antiprotons on neutrons[7] is $\sigma_i(\bar{p}\text{-}n) = 65 \pm 4$ mb at 900 Mev. Since this is in a pure isotopic triplet state also, it should be the same as the inelastic $\bar{n}$-p cross section. Assuming this to be so implies that the inelastic $\bar{n}$-p cross section not due to annihilation is 20 ± 7 mb. The proton-proton interaction is also a pure isotopic triplet state, and its inelastic cross section at 900 Mev is about 25 ± 5 mb.[22]

The total charge-exchange cross section into neutral particles for antiprotons of 925 Mev laboratory kinetic energy is $\sigma_{ce} = 7.8 \pm 0.6$ mb,[17] and is in agreement with previous counter results.[3,4] This result contains an inelastic part due to Reaction (2), which from statistical-model arguments, was estimated to be about 1 mb, or 13% of the total 0-prong antineutron production cross section. The angular differential cross section for charge exchange in Fig. 7 also contains this 13% inelastic contribution. The inelastic differential cross section is probably similar to that for Reaction (6), $\bar{p} + p \rightarrow \bar{n} + p + \pi^-$, which is not peaked as strongly in the

forward direction (see Fig. 9). The antineutron went backward in the center-of-mass frame in four events of the 0-prong $\bar{n}$ production (see Fig. 7). Since there are estimated to be 5 or 6 false associations, some or all of the backward events may be false associations. Some of these backward events could also be due to Reaction (2), the inelastic charge-exchange mode.

ACKNOWLEDGMENTS

We wish to thank the many people of the Lawrence Radiation Laboratory who have aided in the above work. Dr. Sherwood Parker was in charge of the spectrometer alignment, and Mr. Jim Carroll helped with the operation of the electronics and with the preliminary data analysis.

The experimental setup was under the direction of Prof. M. Lynn Stevenson of Prof. Alvarez's group. Donald Gow headed the group operating the bubble chamber, and Dr. Edward Lofgren, the group operating the Bevatron. The accelerator technicians under Don Bliss constructed the counters, and Dick Mack and Horace Jackson of the counter development group aided in designing and maintaining some of the special electronic equipment. Finally, there were many film scanners, film measurers, and IBM 704 programmers who helped in the data reduction. To all these people we express our sincere thanks.

APPENDIX

Statistical-Model Predictions

Several calculations[23-29] have been made of the pion multiplicity in nucleon-antinucleon annihilation according to the Fermi statistical model. The original form for the phase space associated with each pion, $\Omega d^3 \underline{p}$, suggested by Fermi,[23] was not Lorentz-invariant. Numerical evaluation of the phase-space integrals, however, can be greatly simplified if the covariant form $\frac{\mu\Omega}{\omega} d^3 \underline{p}$ is used.[26-29] Here Ω, ω, $\underline{p}$, and μ are, respectively, the interaction volume, energy, momentum, and mass of the pion. This modification seems plausible on the basis of field theory. This covariant form is actually the expression obtained from the covariant S-matrix theory, if it is assumed that the S matrix for the emission of n pions is independent of the energies and momenta of the emitted pions. In view of the crude nature of the Fermi model, such a simple modification may not be unreasonable. For these reasons the covariant form for the phase space was used.

With no consideration of selection rules and assuming that the matrix element for nucleon-antinucleon annihilation is constant, one obtains, for the transition probability for a state of n pions in an isotopic spin state I,

$$S_n(I) = A \frac{G(I)}{n!} \frac{(\mu\Omega)^n}{(2\pi)^{3n}} T_n(E). \qquad (A\text{-}1)$$

The presentation here follows that of Desai,[28] where $\hbar = c = 1$, G(I) is the isotopic spin weight factor, A is a constant independent of n, and $T_n(E)$ is the covariant phase-space integral in the center-of-mass frame at total energy E.

$$T_n(E) = \int \prod_{i=1}^{n} \frac{d^3 \underline{p}_i}{\omega_i} \delta\left(E - \sum_{i=1}^{n} \omega_i\right) \delta\left(\sum_{i=1}^{n} \underline{p}_i\right). \qquad (A\text{-}2)$$

For a particular n and E the only variable parameter in $S_n(I)$ is Ω, the interaction volume. Convenient variation of this parameter was achieved by setting $\Omega = \lambda\Omega_0$, where $\Omega_0 = \frac{4}{3}\pi\left(\frac{1}{\mu}\right)^3$, ($\hbar = c = 1$). Thus Ω_0 is the volume of a sphere with a radius of one pion Compton wavelength.

Equation (A-2) can be written

$$T_n(E) = 4\pi \int p_1 \, d\omega_1 \left[\int \prod_{i=2}^{n} \frac{d^3 p_i}{\omega_i} \, \delta\left(E - \omega_1 - \sum_{i=2}^{n} \omega_i\right) \delta\left(\underline{p}_1 + \sum_{i=2}^{n} \underline{p}_i\right) \right], \qquad (A\text{-}3)$$

where $d^3\underline{p} = 4\pi p^2 \, dp = 4\pi \, \omega \, p \, d\omega$.

Since $d^3\underline{p}/\omega$ is Lorentz-invariant, if we transform to the particular Lorentz frame primed variables where

$$\sum_{i=2}^{n} \underline{p}'_i = 0, \text{ and } \sum_{i=2}^{n} \omega_i' = E',$$

The square-bracketed portion of Eq. (A-3) becomes:

$$\left[\int \prod_{i=2}^{n} \frac{d^3 p_i'}{\omega_i'} \, \delta\left(E' - \sum_{i=2}^{n} \omega_i'\right) \delta\left(\sum_{i=2}^{n} \underline{p}_i'\right) \right], \qquad (A\text{-}4)$$

which is just $T_{n-1}(E')$, according to Eq. (A-2). Hence, the recursion relation is

$$T_n(E) = 4\pi \int_{\mu}^{\bar{\omega}_1} p_1 \, d\omega_1 \, T_{n-1}(E'). \qquad (A\text{-}5)$$

From Lorentz invariance, $\left(\sum_{i=2}^{n} \omega_1\right)^2 - \left(\sum_{i=2}^{n} \underline{p}_i\right)^2$ = constant in all coordinate systems. Thus we have $(E')^2 - 0 = (E - \omega_1)^2 = p_1^2$, defining E'. The maximum energy $\bar{\omega}_1$ assumed by particle 1 corresponds to $E' = (n-1)\mu$. The upper limit to the integral in Eq. (A-5) is then $\bar{\omega}_1 = \frac{E^2 - n(n-2)\mu}{2E}$. By means of Eq. (A-5), $T_n(E)$ can be evaluated successively, where finally

$$T_2(E0 = 2\pi (1 - 4\mu^2/E^2)^{1/2}. \qquad (A\text{-}6)$$

Thus for a particular energy E and volume factor λ the relative probabilities for producing various numbers of pions can be calculated.

If it is assumed that all individual channels contribute, with the same weight, to the total transition probability, the branching ratios for the various modes can be calculated for each number of pions emitted. For example, in the case in which n = 3 there are two modes of antineutron-proton annihilation:

$$\bar{n} + p \rightarrow 2\pi^0 + \pi^+,$$
$$\bar{n} + p \rightarrow 2\pi^+ + \pi^-.$$

The branching ratios have been calculated by Pais[30] as 2/5 and 3/5, respectively.

The values of $T_n(E)$ calculated by Desai[28] and the branching ratios evaluated by Pais[30] were used to calculate the fraction of annihilations occurring by each mode, for values of n up to n = 8 and for various values of λ and E. (The annihilations with n greater than 8 are less than 1% for the energies considered). These calculations were performed by a computer program. This program also determined the average pion multiplicity, the ratio of the number of charged pions to neutral pions, and the fraction of annihilations giving 1-, 3-, 5-, and 7-prongs (a 1-prong corresponds to one charged pion, a π^+). In addition, the number

$$K(E) = \frac{1}{\text{fraction of } 3 + 5 + 7 \text{ prongs}}, \qquad \text{(A-7)}$$

which is the correction for unobservable 1-prong annihilations, was also calculated. In Fig. 5, K is plotted as a function of antineutron laboratory-frame kinetic energy for $\lambda = 5$.

The ratio of the number of 5-prong to 3-prong annihilations as a function of antineutron laboratory-frame kinetic energy is plotted in Fig. 4 for various values of λ.

The momentum distribution for one of the pions in an annihilation producing n pions can be obtained by simply not performing the first integral in Eq. (A-3),

$$\frac{dT_n(E)}{d\,p_1} = 4\pi \frac{p_1^{\,2}}{\omega_1} \left[\int \prod_{i=2}^{n} \frac{d^3 p_i}{\omega_i} \delta \left(E - \omega_1 - \sum_{i=2}^{n} \omega_i \right) \delta \left(\underline{p}_1 + \sum_{i=2}^{n} \underline{p}_i \right) \right]. \qquad \text{(A-8)}$$

From Eqs. (A-1) and (A-8), $[\, dS_n(E)]/\, d\, p_1$ can be obtained. The momentum distribution for pions in a 3-prong annihilation is then given by

$$\frac{dS\ (3\text{-prong})}{dp_1} = \sum_{n \geq 3} f_{3,n} \frac{dS_n(E)}{dp_1}\ , \qquad \text{(A-9)}$$

where $f_{3,n}$ is the fraction of the n pion annihilations giving three charged pions. A similar relation gives the momentum distribution of pions in 5-prong annihilations.

Equation (A-8) was evaluated for values of n up to n = 8 by a computer program. Momentum distributions calculated for $\lambda = 5$ and $\lambda = 6$ and an anti-neutron laboratory kinetic energy of 900 Mev are given in Figs. 11 and 12 for 3-prong and 5-prong annihilations, respectively. The curves have been normalized to the numbers of pions observed.

FOOTNOTES AND REFERENCES

* Work done under the auspices of the U. S. Atomic Energy Commission.

† Present address: Aerojet General Nucleonics, San Ramon, California.

‡ Present address: Goddard Space Center, Greenbelt, Maryland.

1. B. Cork, G. R. Lambertson, O. Piccioni, and W. A. Wenzel, Phys. Rev. 104, 1193 (1956).
2. C. A. Coombes, B. Cork, W. Galbraith, G. R. Lambertson, and W. A. Wenzel, Phys. Rev. 112, 1303 (1958).
3. T. Elioff, L. Agnew, O. Chamberlain, H. M. Steiner, C. Wiegand, and T. Ypsilantis, Phys. Rev. Letters 3, 285 (1959).
4. R. Armenteros, C. A. Coombes B. Cork, G. R. Lambertson, and W. A. Wenzel, Phys. Rev. 119, 2068 (1960).
5. J. Button, T. Elioff, E. Segrè, H. M. Steiner, R. Weingart, C. Wiegand, and T. Ypsilantis, Phys. Rev. 108, 1557 (1957).
6. L. E. Agnew, Jr., T. Elioff, W. B. Fowler, L. Gilly, R. L. Lander, L. Oswald, W. M. Powell, E. Segrè, H. Steiner, H. White, C. Wiegand, and T. Ypsilantis, Phys. Rev. 110, 994 (1958); L. E. Agnew, Jr., T. Elioff, W. B. Fowler, R. L. Lander, W. M. Powell, E. Segrè, H. M. Steiner, H. S. White, C. Wiegand, and T. Ypsilantis, Phys. Rev. 118, 1371 (1960).
7. T. Elioff, L. Agnew, O. Chamberlain, H. M. Steiner, C. Wiegand, and T. Ypsilantis, Antiproton-Nucleon Cross Sections from 0.5 to 1.0 Bev, Phys. Rev. (submitted for publication)[based on: T. Elioff (Ph. D. Thesis), Lawrence Radiation Laboratory Report UCRL-9288, July 1960].
8. M. Lynn Stevenson, in Ninth International Annual Conference on High Energy Physics, Kiev, 1959 (Academy of Sciences, Moscow, 1960).

9. J. Button, P. Eberhard, G. R. Kalbfleisch, J. E. Lannutti, G. R. Lynch, B. C. Maglic, M. L. Stevenson, and N. H. Xuong, Phys. Rev. 121, 1788 (1961).

10. J. D. Gow and A. H. Rosenfeld, Berkeley 72-Inch Hydrogen Bubble Chamber, in Proceedings of the International Conference on High Energy Accelerators and Instrumentation (CERN, Geneva, 1959), pp. 435-439.

11. The Franckenstein measuring projector was designed and built by Jack V. Franck and his group. A brief description of this machine is contained in the second item of reference 12.

12. Developed by Frank T. Solmitz, R. Harvey, and W. Humphrey; A description of the PANG program, Alvarez Group Memo 111, Sept. 18, 1959, and Memo 115, Oct. 25, 1959, Lawrence Radiation Laboratory; A. H. Rosenfeld, Digital Computer Analysis of Data from Hydrogen Bubble Chambers at Berkeley, in Proceedings of the International Conference on High Energy Accelerators and Instrumentation (CERN), Geneva, 1959), pp. 533-539.

13. P. Falk-Vairant and G. Valladas, Results in Pion-Proton Scattering Near the Higher Resonances, in Proceedings of the 1960 Annual International Conference on High Energy Physics at Rochester (Interscience Publishers, Inc., New York, 1960), pp. 38-45; J. C. Brisson, P. Falk-Vairant, J. P. Merlo, P. Sonderegger, R. Turlay, and G. Valladas, Measurement of the Total Cross Section for π^--p Charge Exchange from T_π = 0.4 Gev to T_π = 1.5 Gev, in Proceedings of the 1960 Annual International Conference on High-Energy Physics at Rochester (Interscience Publishers, Inc., New York, 1960), pp. 191-193.

14. This was obtained by extrapolating the curves for the cross section of the reactions $\pi^- + p \rightarrow \pi^0 + n$ and $\pi^- + p \rightarrow 2\pi^0 + n$, with the sum of the cross sections equal to 4.75 mb; see P. Falk-Vairant, in Proceedings of Conference on Strong Interactions, University of California, Berkeley, Dec. 27-29, 1960, published in Revs. Modern Phys. 33, No. 3 (July 1961). See also reference 13.

15. Z. Koba and G. Takeda, Progr. Theoret. Phys. (Kyoto) 19, 269 (1958).

16. Gerald R. Lynch, Revs. Modern Phys. 33, 395 (1961).

17. If the statistical-model predictions for 0-prong annihilation are used, instead of the method employed in Sec. III-D, the 0-prong production of antineutron is reduced to 1473. The core radius a then becomes 0.959f, which gives an anti-neutron annihilation cross section at 900 Mev of $\sigma_a(\bar{n}p)$ = 50 mb. The charge-exchange cross sections become σ_{ce}(0-prong) = 7.1 mb; $\sigma(p+p \rightarrow \bar{n}+p+\pi^-)$ = 0.9 mb.

18. T. Elioff, L. Agnew, O. Chamberlain, H. M. Steiner, C. Wiegand, and T. Ypsilantis, Phys. Rev. Letters 3, 285 (1959).

19. Originally developed by A. Rosenfeld, J. Snyder, and J. P. Berge for treatment of K-meson interactions. A. H. Rosenfeld and J. N. Snyder, Digital Computer Analysis of Data from Bubble Chambers. IV. The Kinematic Analysis of Complete Events, Rev. Sci. Instr. (in press) (Lawrence Radiation Laboratory Report UCRL-9098, Feb. 1960); J. P. Berge, F. T. Solmitz, and H. D. Taft, Rev. Sci. Instr. 32, 538 (1961).

20. G. Goldhaber, W. Fowler, S. Goldhaber, T. Hoang, T. Kalogeropoulos, and W. Powell, Phys. Rev. Letters 3, 181 (1959).

21. G. Goldhaber, S. Goldhaber, W. Lee, and A. Pais, Phys. Rev. 120, 300 (1960).

22. W. N. Hess, Revs. Modern Phys. 30, 368 (1958).

23. E. Fermi, Progr. Theoret. Phys. (Kyoto) 5, 570 (1950).

24. S. Z. Belenkii and I. S. Rosenthal, J. Exptl. Theoret. Phys. (U.S.S.R.) 3, 786 (1956).

25. G. Sudarshan, Phys. Rev. 103, 777 (1956).

26. P. P. Srivastava and G. Sudarshan, Phys. Rev. 110, 765 (1958).

27. M. Neuman, Statistical Models for High Energy Nuclear Reactions I and II, Separate Do Vol. 31, No. 3 and No. 4, Anais de Academia Brasileira De Ciencias, Rio de Janeiro, 1959.

28. B. R. Desai, Phys. Rev. 119, 1390 (1960).

29. T. E. Kalogeropoulos, A Study of the Antiproton Annihilation Process in Complex Nuclei (Ph. D. Thesis) Lawrence Radiation Laboratory Report UCRL-8677, March 1959 (unpublished).

30. A. Pais, Ann. Phys. 9, 548 (1960).

Table I. List of interaction types in terms of final-state charged-particle tracks.

0-Prongs		
$\bar{p} + p \rightarrow \bar{n} + n$	charge exchange	(1)
$\rightarrow \bar{n} + n + \pi^0$	inelastic charge exchange	(2)
$\rightarrow \pi^0$'s + K^0's	annihilation	(3)
$\pi^- + p \rightarrow \pi^0 + n$	charge exchange	(4)
$\rightarrow \pi^0 + \pi^0 + n$	inelastic scatter	(5)
2-, 4-, 6-, 8-Prongs		
$\bar{p} + p \rightarrow \bar{n} + p + \pi^-$	inelastic charge exchange	(6)
$\rightarrow \bar{p} + p$	elastic scatter	(7)
$\rightarrow \pi$'s + K's	annihilation	(8)
$\pi^- + p \rightarrow \pi^- + p$	elastic scatter	(9)
$\rightarrow \pi^+ + \pi^- + n$	inelastic scatter	(10)
$\rightarrow \pi^- + p + \pi^0$	inelastic scatter	(11)
1-, 3-, 5-, 7-Prongs		
$\bar{n} + p \rightarrow \bar{n} + p$	elastic scatter	(12)
$\rightarrow \pi$'s + K's	annihilation	(13)
$n + p \rightarrow n + p$	elastic scatter	(14)
$\rightarrow n + p + \pi$'s	inelastic scatter	(15)
$\rightarrow p + p + \pi$'s	inelastic scatter	(16)
$\rightarrow n + n + \pi$'s	inelastic scatter	(17)

FIGURE LEGENDS

Fig. 1. Bubble chamber photograph of an antiproton charge exchange into an antineutron. The antineutron then annihilated into five charged pions.

Fig. 2. Bubble chamber photograph of the reaction $\bar{p} + p \rightarrow \bar{n} + p + \pi^-$. The $\bar{n}$ then annihilated into three charged pions (arrow).

Fig. 3. Energy distribution of antineutrons produced by 0-prong charge exchange (117 events).

Fig. 4. Statistical-model predictions for the ratio R of the number of 5-prong to 3-prong annihilation stars.

Fig. 5. The correction factor for 1-prong annihilations, K, as a function of antineutron kinetic energy. $\lambda = 5$.

Fig. 6. The number of antineutrons produced by 0-prongs, $N_0^{\bar{n}}$, as a function of the core radius, a.

Fig. 7. The differential cross section for charge exchange as a function of $\cos\Theta_{\bar{n},\bar{p}}^{\text{c.m.}}$ is shown in the lower figure. The raw data from which this was reduced is shown above.

Fig. 8. Energy distribution of antineutrons produced by 2-prong charge exchange (19 events).

Fig. 9. Center-of-mass angular distribution of the particles in the reaction $\bar{p} + p \rightarrow \bar{n} + p + \pi^-$ relative to the $\bar{p}$ direction (20 events).

Fig. 10. Azimuthal angular distribution of the $\bar{n}$ about the $\bar{p}$ direction in the reaction $\bar{p} + p \rightarrow \bar{n} + p + \pi^-$ (20 events). Zero azimuthal angle is defined by the plane of the proton and the antiproton.

Fig. 11. Center-of-mass momentum distribution of charged pions in 3-prong annihilation stars.

Fig. 12. Center-of-mass momentum distribution of charged pions in 5-prong annihilation stars.

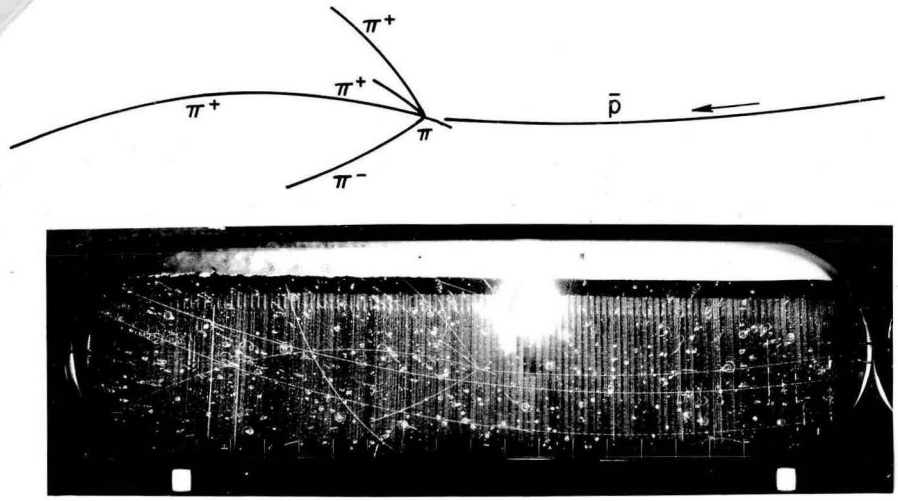

Fig. 1

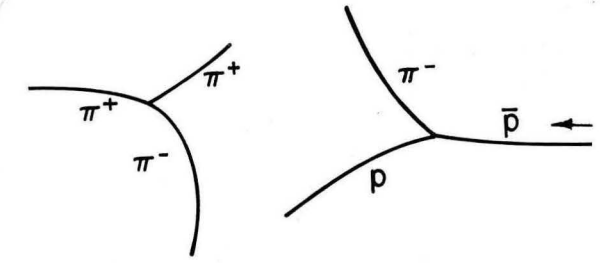

Fig. 1

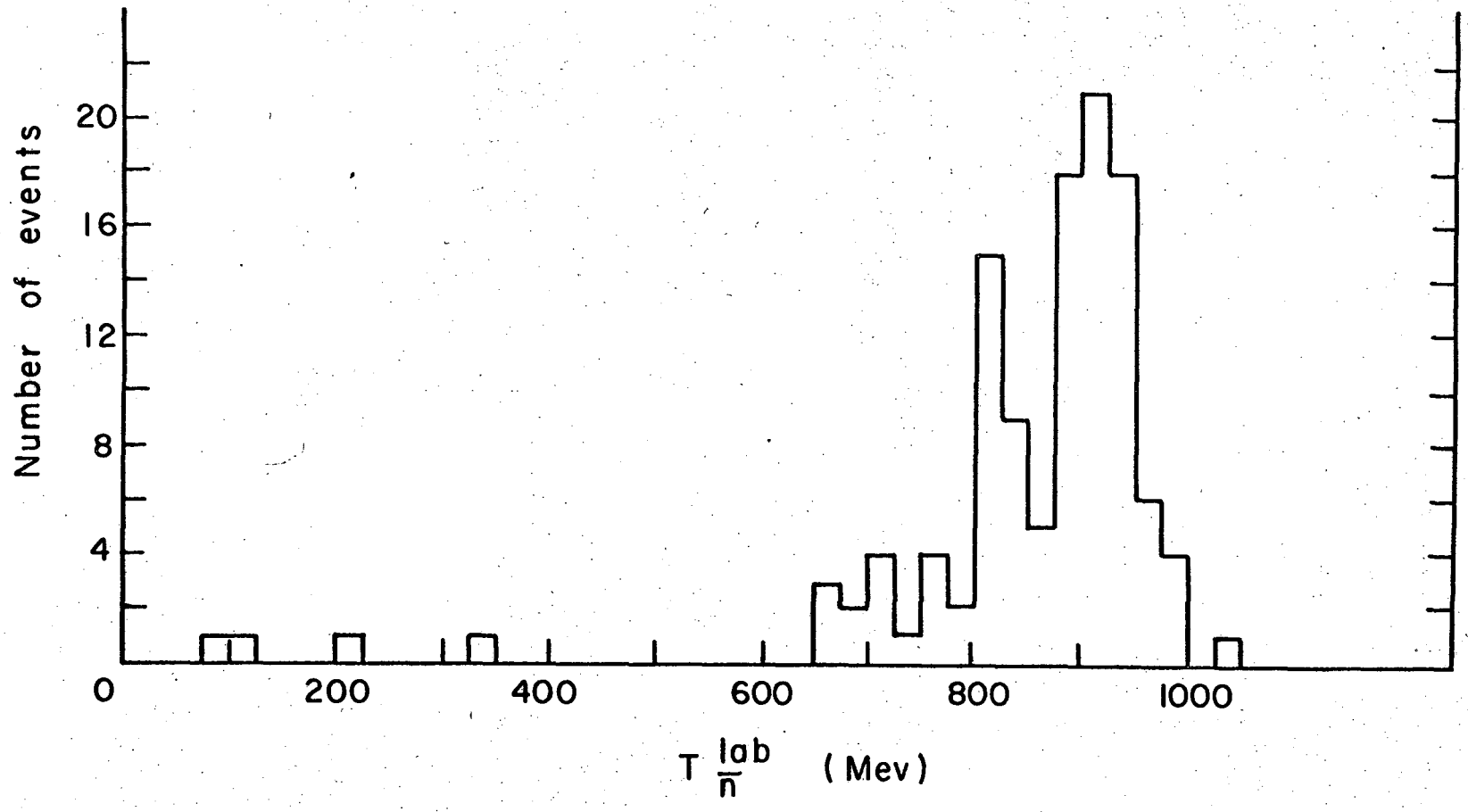

MU-23150

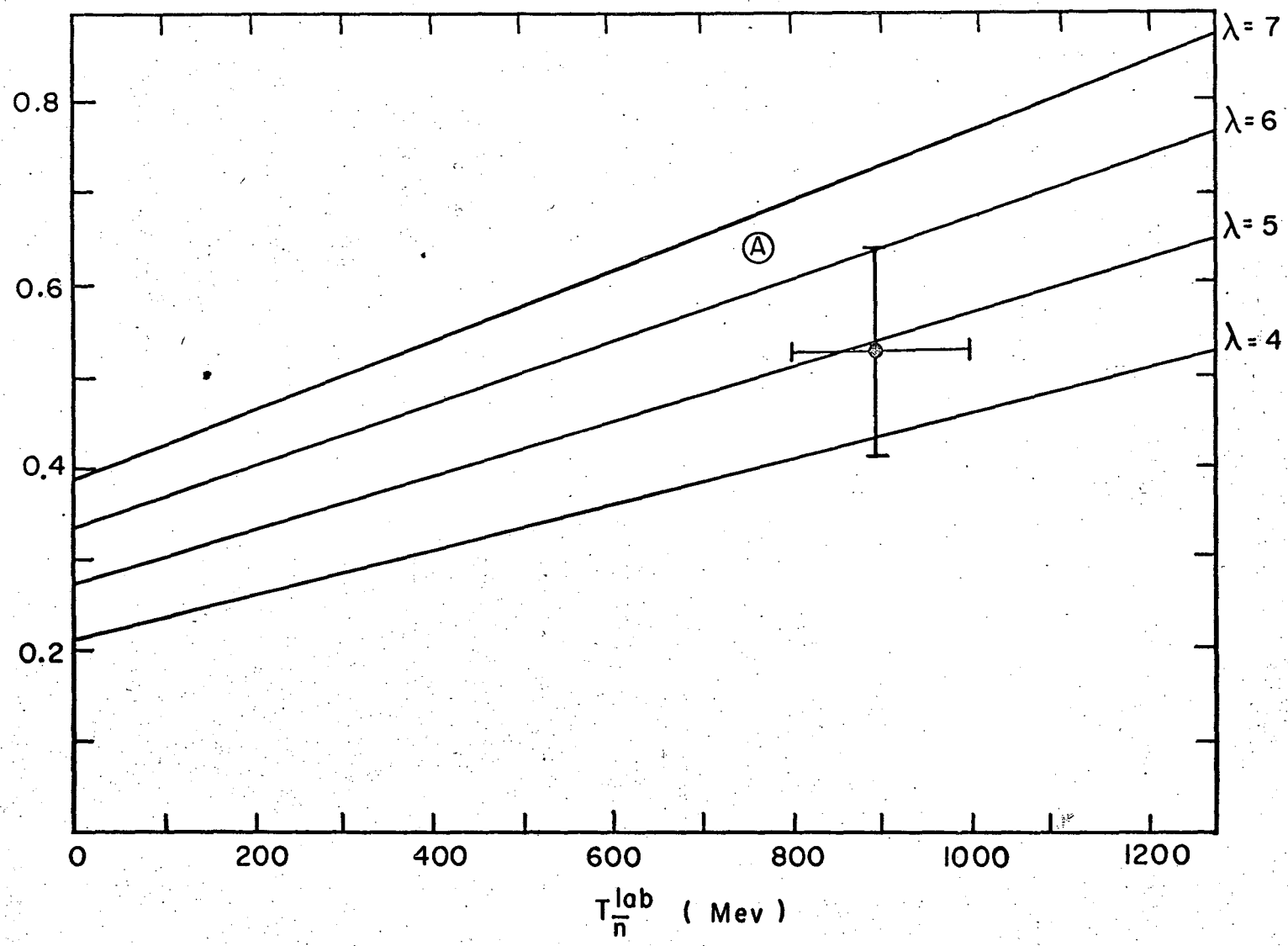

MU-23156

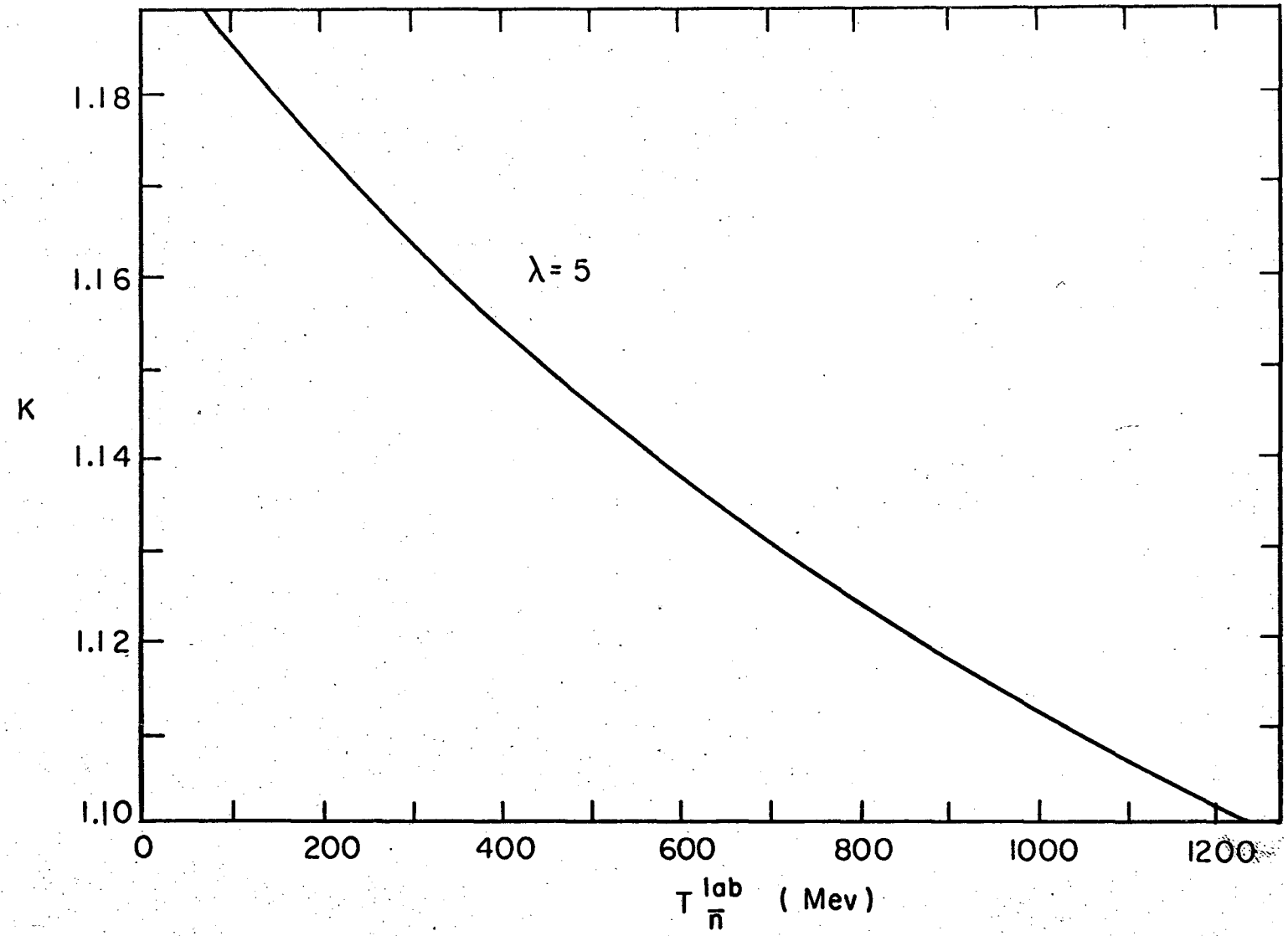

MU-23155

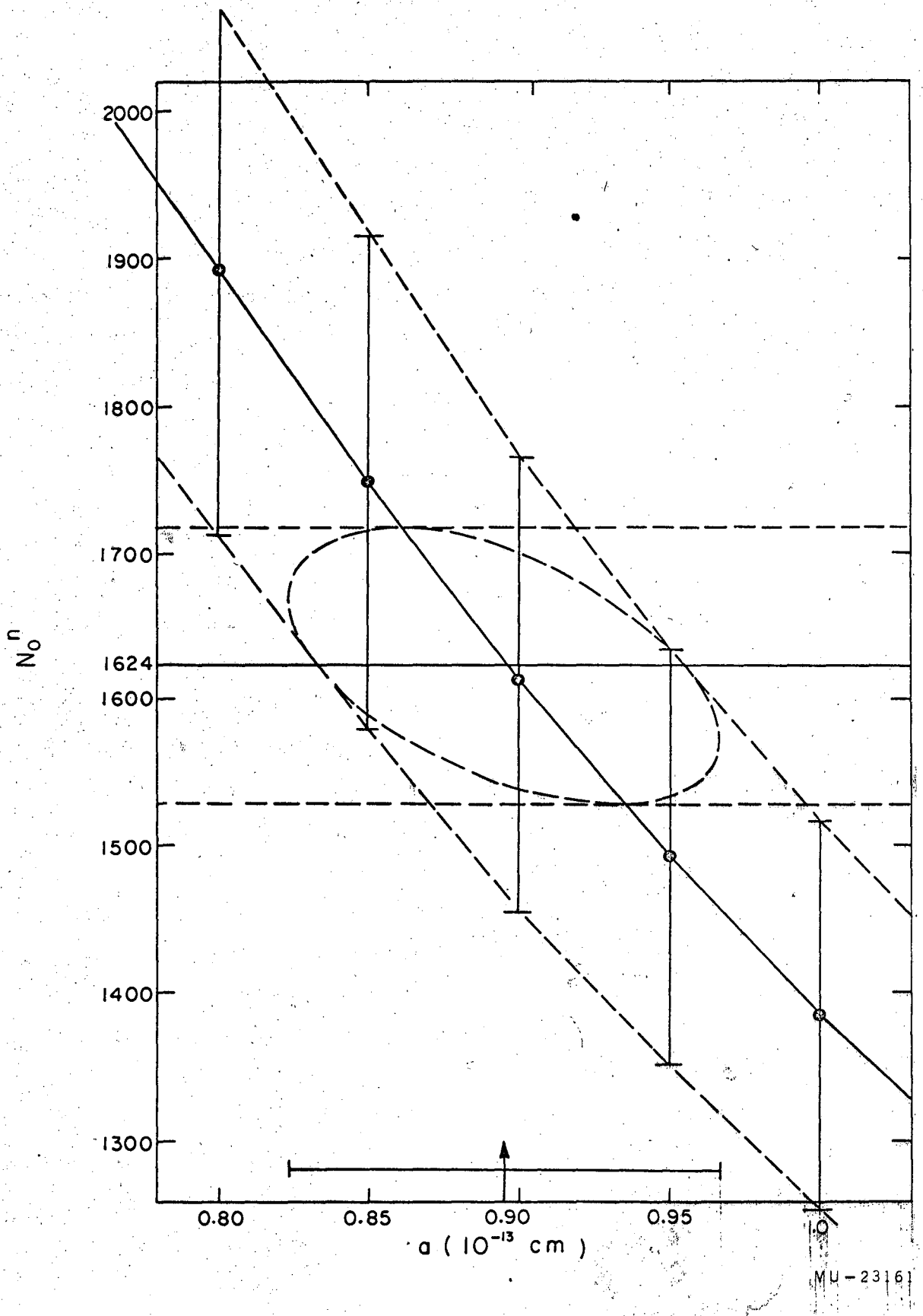
2000
1900
1800
1700
1624
1600
1500
1400
1300
N_0^n
0.80
0.85
0.90
0.95
1.0
a (10^{-13} cm)
MU-23161

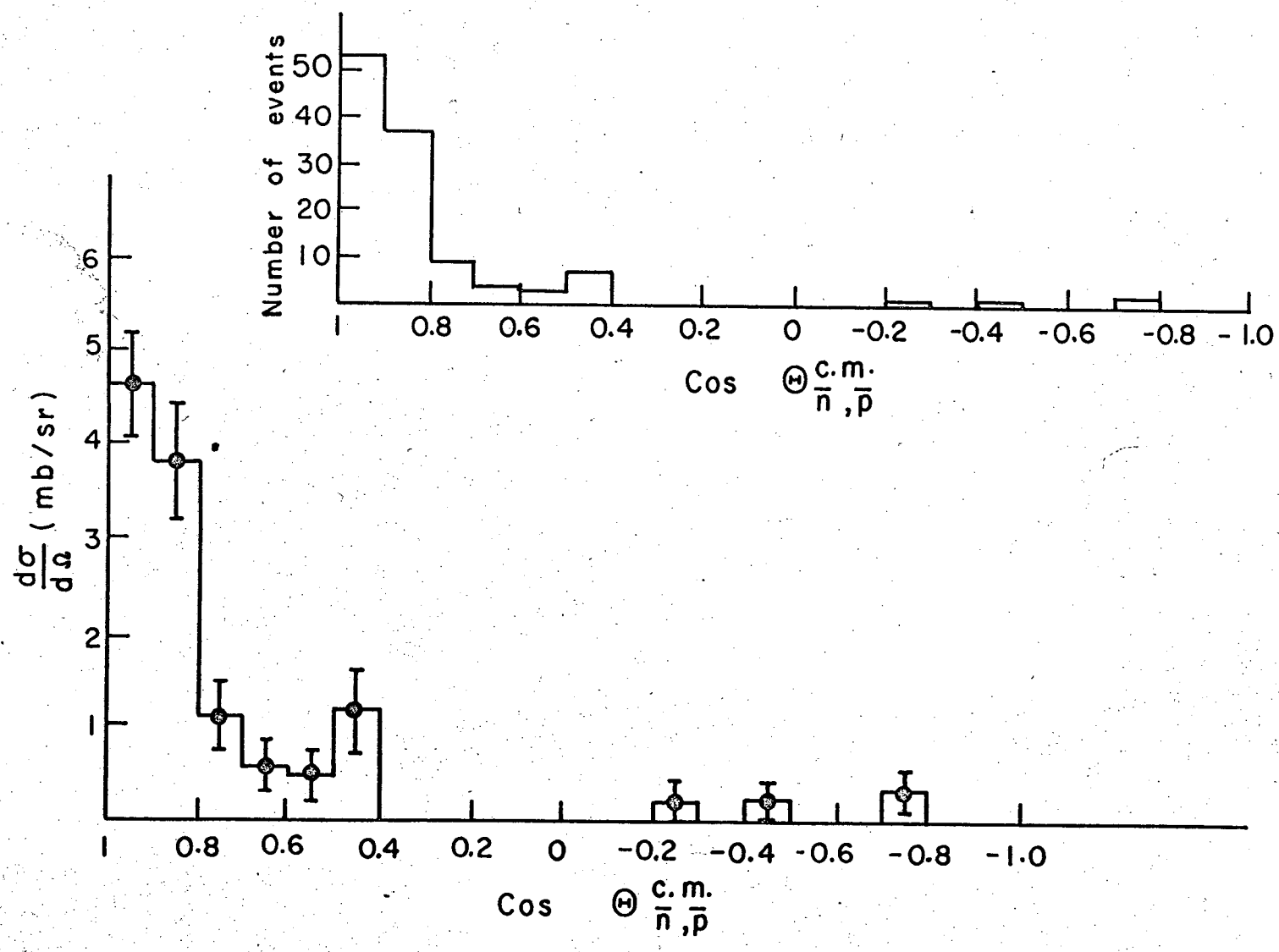
Number of events
50
40
30
20
10
1
0.8
0.6
0.4
0.2
0
-0.2
-0.4
-0.6
-0.8
-1.0
Cos Θ c.m. n̄, p̄
dσ/dΩ (mb/sr)
6
5
4
3
2
1
1
0.8
0.6
0.4
0.2
0
-0.2
-0.4
-0.6
-0.8
-1.0
Cos Θ c.m. n̄, p̄

MU-23148

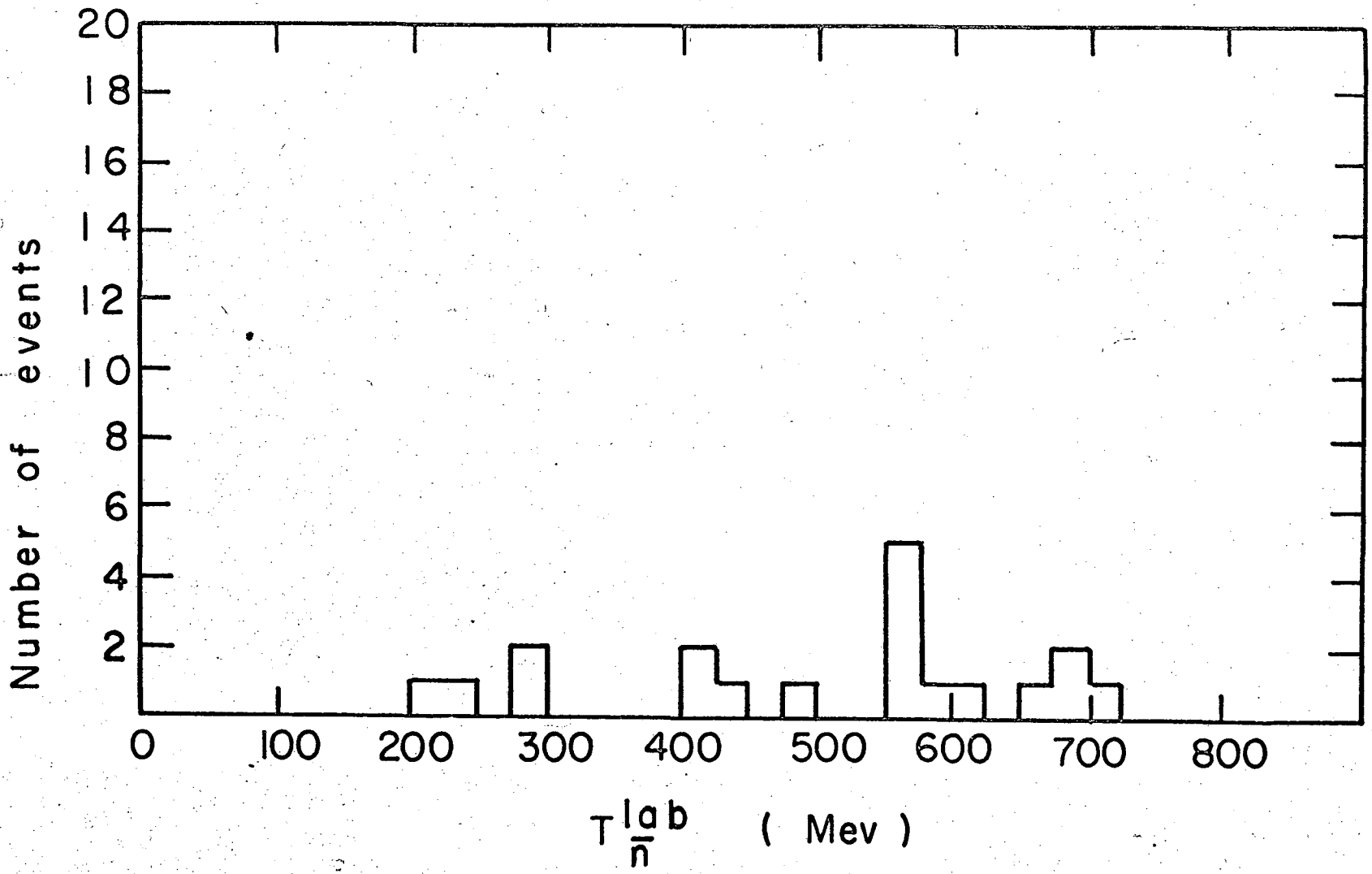
Number of events
20
18
16
14
12
10
8
6
4
2
0
100
200
300
400
500
600
700
800
$T_{\bar{n}}^{lab}$ (Mev)

MU-23159

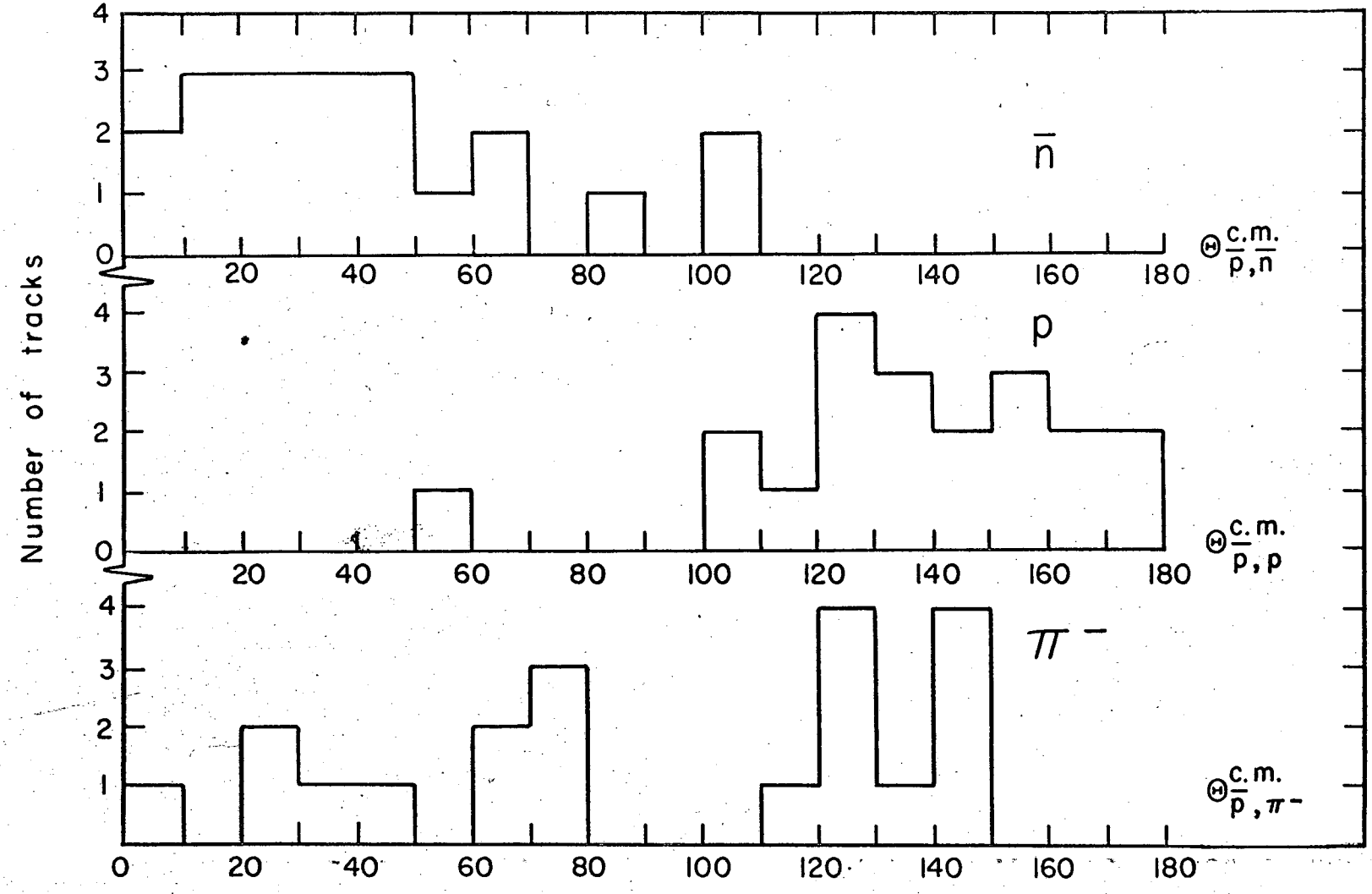
Number of tracks
$\bar{n}$
$\Theta^{c.m.}_{\bar{p},\bar{n}}$
p
$\Theta^{c.m.}_{\bar{p},p}$
π^-
$\Theta^{c.m.}_{\bar{p},\pi^-}$
0
20
40
60
80
100
120
140
160
180
1
2
3
4

MU-23151

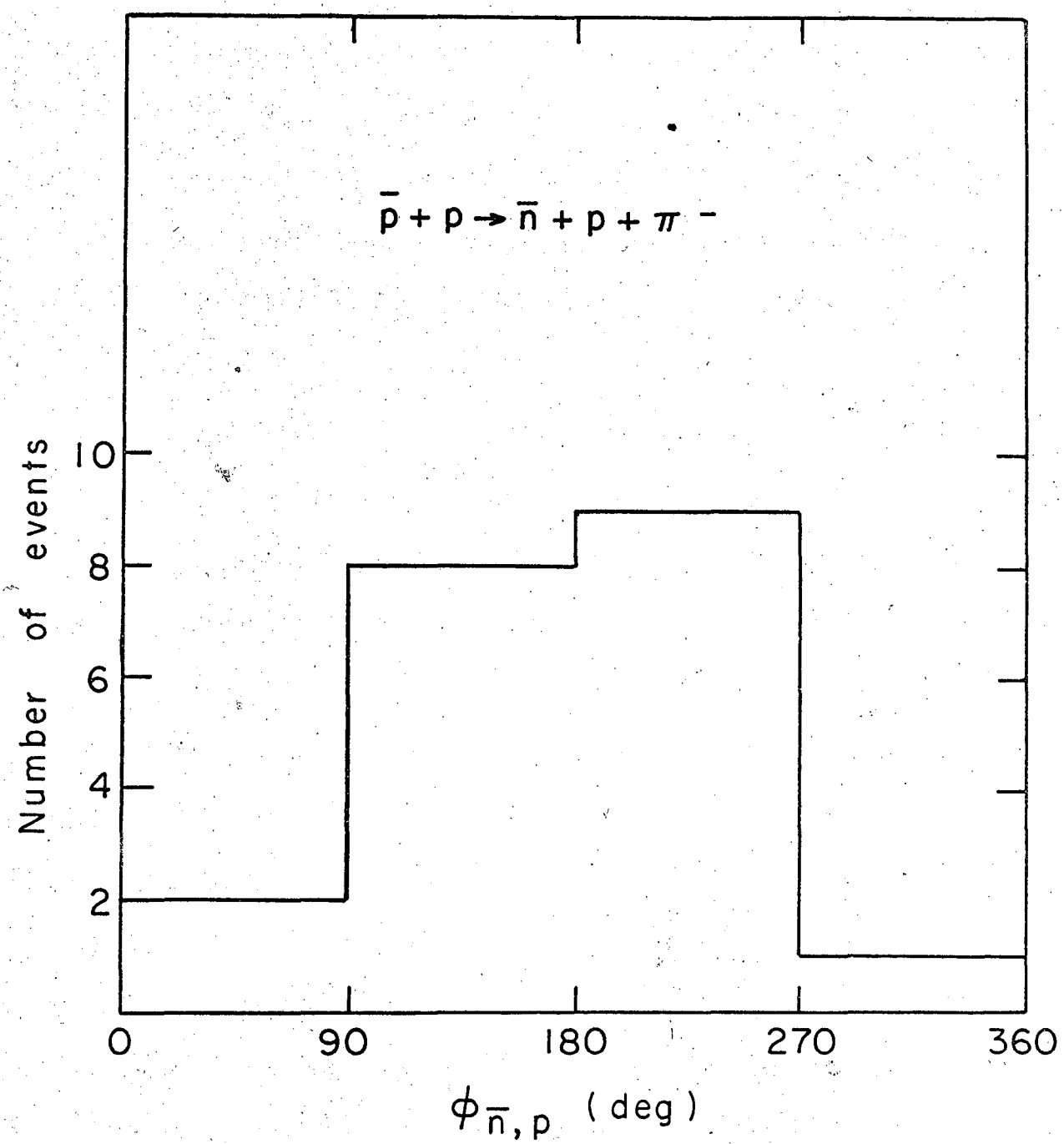
$\bar{p} + p \rightarrow \bar{n} + p + \pi^-$
Number of events
10
8
6
4
2
0
90
180
270
360
$\phi_{\bar{n},p}$ (deg)

MU-23157

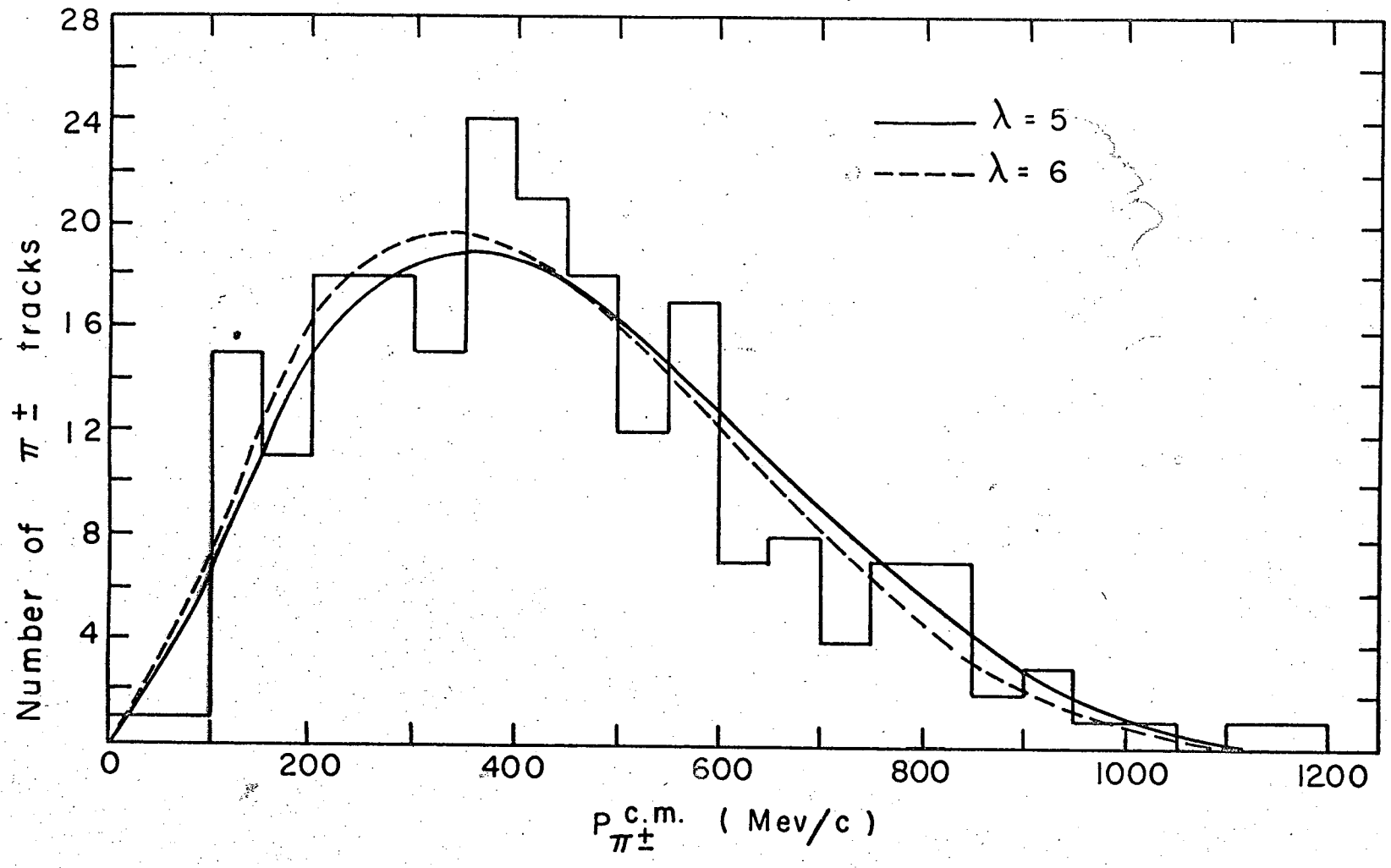
28
24
20
16
12
8
4
0
200
400
600
800
1000
1200
λ = 5
λ = 6
Number of π± tracks
P c.m. π± (Mev/c)

MU-23158

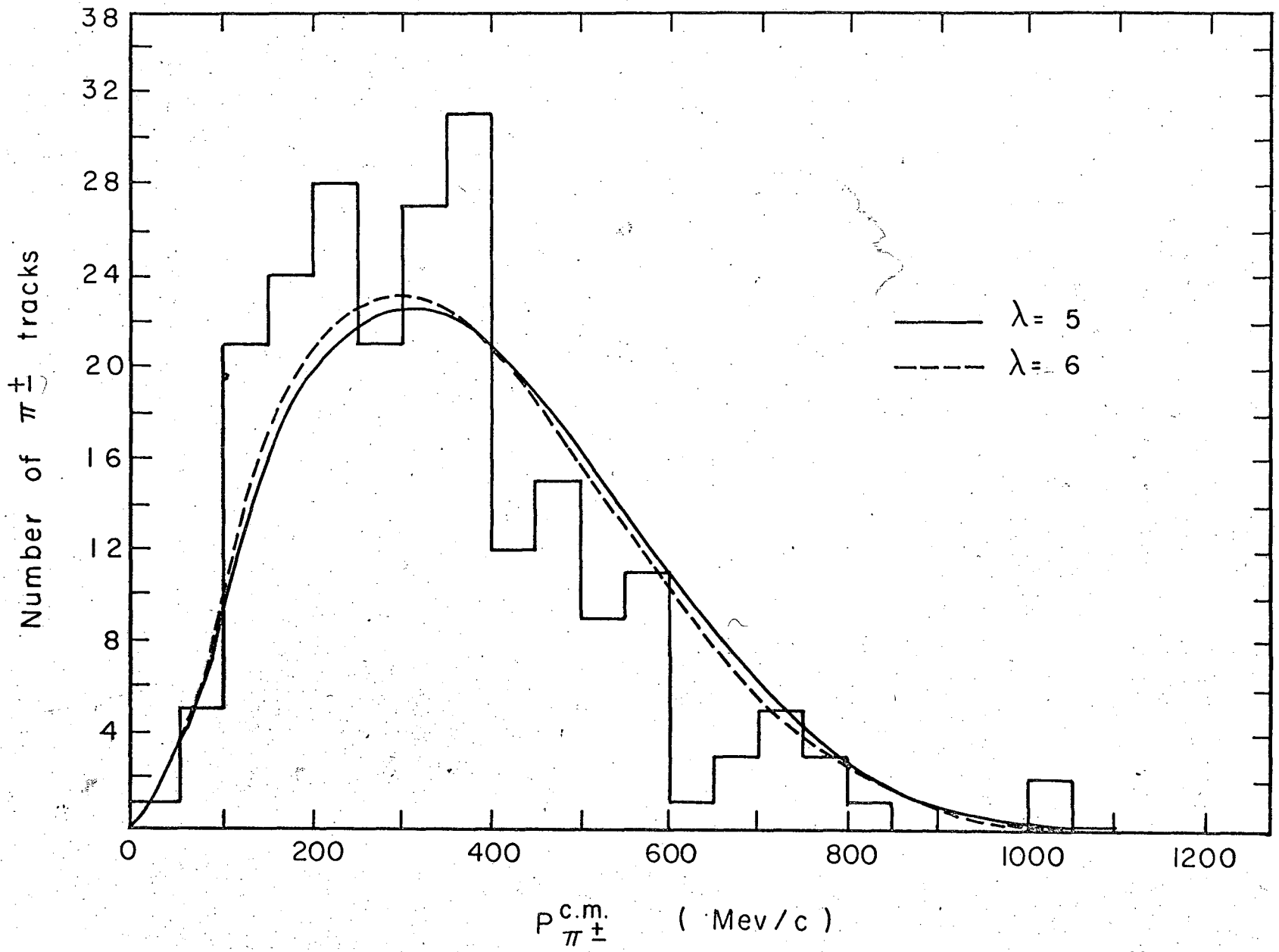
38
32
28
24
20
16
12
8
4
Number of $\pi^{\pm}$ tracks
0
200
400
600
800
1000
1200
$P^{c.m.}_{\pi^{\pm}}$ (Mev/c)
λ= 5
λ= 6

MU-23153